DOI: 10.1002/adma.200600741

Highly Oriented Thin-Film Microdomain Patterns of Ultrahigh Molecular Weight Block Copolymers via Directional Solidification of a Solvent**

By *Jongseung Yoon*, *Wonmok Lee*, and *Edwin L. Thomas**

Self-assembly is rapidly emerging as a simple and effective method for creating large-area functional periodic structures in various nanotechnologies.[1–3] In particular, block copolymers (BCPs) have been considered as promising self-organizing platforms because of their tunability in shape, size, and physical/chemical properties of the domains, with the capability of hosting many types of additives for desirable multifunctional composites.[4] Recently, ultrahigh molecular weight (number average molecular weight, $M_n \sim 10^6$ g mol^{-1}) BCPs possessing a domain size comparable to the wavelength of visible light have received increasing attention as self-assembled photonic materials.[5] 1D, 2D, and 3D photonic crystals for visible frequencies have been successfully demonstrated using lamellar, cylindrical, and double gyroid morphologies of polystyrene-*block*-polyisoprene (PS-*b*-PI) BCPs.[6–8] While most previous work on these photonic BCPs has been limited to relatively thick samples with only modest control over microdomain order, numerous engineering applications such as thin-film waveguides, reflectors, and microcavities for lasing can potentially be achieved from controlled thin-film microstructures of these materials, all of which depend critically on the overall order of the microdomains to meet desired functionalities. Here we demonstrate the excellent control of thin-film microdomain patterns of lamellar- and cylinder-forming ultrahigh molecular weight BCPs (ca. 20 times larger molecular weight than for previously studied block copolymers) over a large area via directional solidification (DS) of a solvent. The ordering behavior of these photonic BCPs via the DS process has been found to be dramatically different from that of directionally solidified conventional molecular weight BCPs. Because of the relatively large domain sizes of ultrahigh molecular weight BCPs, laser scanning confocal microscopy (LSCM) could be used to optically characterize the lamellar and cylindrical thin film structures in 3D space.

The directional solidification of BCPs with benzoic acid (BA) resulted in an excellent orientational control of the self-assembled microdomains over a large area (ca. 100 μm × 100 μm), as shown in the reflection-mode LSCM micrographs. Figure 1a shows the highly oriented lamellar microdomains, SI_{LAM}, oriented such that their intermaterial dividing surfaces (IMDSs) are approximately perpendicular to the fast-growth direction of the BA crystal ($\mathbf{b}_{BA}$, i.e., the crystallographic *b*-axis of the BA crystal). Directional solidification also created well-ordered cylindrical microdomains, SI_{CYL}, in a thin film as shown in Figure 1b, where the PS cylindrical domains are lying in the *xy*-plane and the cylinder axes are perpendicular to $\mathbf{b}_{BA}$. The relative microdomain orientation with respect to the BA growth direction was determined from low-magnification LSCM images, where the fast-growth direction of the BA crystal was readily identified. For example, Figure 1c shows a low-magnification LSCM image of SI_{CYL} in which a long and narrow region represents the highly ordered cylindrical domains aligned normal to the fast-growth direction of BA.

To further explore the BCP thin-film nanostructure, a series of LSCM *xy*-images were taken varying the *z* position (i.e., along the film-thickness direction) to permit 3D image reconstruction. Figure 2 shows the 3D LSCM representations of the SI_{LAM} and SI_{CYL} thin films and corresponding schematics. Interestingly, the lamellar microdomains are tilted by about 60° to $\mathbf{b}_{BA}$ as shown in Figure 2a. 3D imaging of the SI_{CYL} thin film revealed that it is composed of approximately four layers of hexagonally packed PS cylinders in the film thickness direction as shown in Figure 2b. From the side view of the SI_{CYL} thin film (*yz*-plane), the second and fourth layers of cylinders appear brighter since the first and third layers of cylinders are offset from the focal plane. The hexagonal packing of cylindrical domains in the *xz*-plane was also confirmed by *xy*-scans of the film at varying *z*-locations, which clearly shows alternating

[*] Prof. E. L. Thomas, Dr. J. Yoon, Dr. W. Lee[+]
Department of Materials Science and Engineering
Massachusetts Institute of Technology
Cambridge, MA 02139 (USA)
E-mail: elt@mit.edu
Prof. E. L. Thomas
Institute for Soldier Nanotechnologies
Massachusetts Institute of Technology
Cambridge MA 02139 (USA)

[+] Present address: Samsung Advanced Institute of Technology, Yongin-si, Gyeonggi-do, Korea.

[**] J. Yoon and W. Lee contributed equally to this work. The authors thank their respective financial sources; J. Yoon, the National Science Foundation for financial support under Grant No. DMR-0308133; W. Lee, the U.S. Air Force Defense University Research Initiative on Nanotechnology in conjunction with the University of Buffalo; E. L. Thomas, the above two agencies and the Institute for Soldier Nanotechnologies of the U.S. Army Research Office. The authors gratefully acknowledge Prof. Timothy Swager at MIT for help with LSCM facility, Dr. Peter DeRege for providing the high molecular weight cylinder-forming block copolymer (SI_{CYL}) used in this study, and Prof. Cheolmin Park at Yonsei University (Korea) for useful discussions. Supporting Information is available online from Wiley InterScience or from the author.

ADVANCED MATERIALS

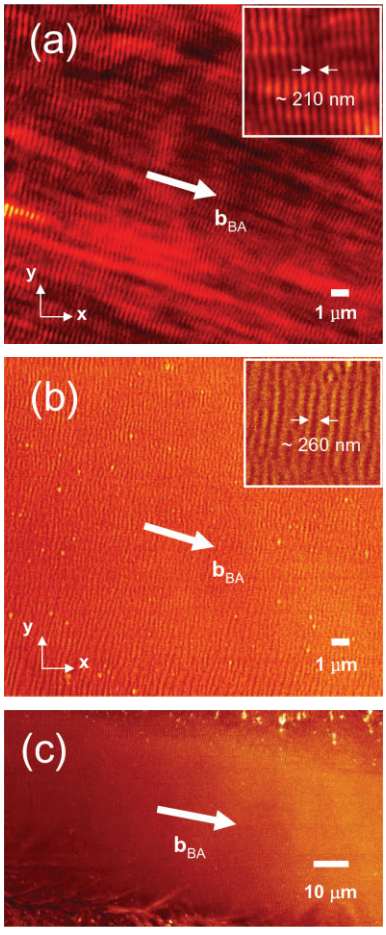

Figure 1. Reflection mode LSCM images (*xy*-scan) of PS-*b*-PI BCPs showing highly oriented a) lamellar and b) cylindrical microdomains in thin films obtained from a directional solidification process with benzoic acid (BA). Intermaterial dividing surfaces (IMDSs) are principally aligned perpendicular to the fast growing direction of benzoic acid (the *b*-axis of the BA crystal) in both lamellar and cylindrical samples. The insets are high-magnification images of a) the edge-on lamellae and b) the in-plane cylinders, in which the lamellar periodicity ($d_{LAM} \sim 210$ nm) and the intercylinder spacing ($d_{CYL} \sim 260$ nm) are shown. c) A low-magnification LSCM image (*xy*-scan) of SI_{CYL} showing the relative orientation of cylindrical microdomains with respect to the fast-growth direction of the BA crystal.

registration of cylindrical domains at different depths (Supporting Information available). The elongated shape of the cylindrical cross section in the *xz*-plane can be attributed to the limited axial resolution of LSCM.[9,10]

An intriguing phenomenon in the DS process found in this study is the molecular-weight dependence of the BCP microdomain orientation with respect to the fast-growth direction of BA. According to our previous studies using conventional molecular weight lamellar and cylindrical BCPs ($M_n \sim 5 \times 10^4$ g mol^{-1}), the IMDSs are predominantly oriented parallel to $\mathbf{b}_{BA}$, that is, the lamellar normal was aligned perpendicular to $\mathbf{b}_{BA}$ and the cylinder axis was aligned parallel to $\mathbf{b}_{BA}$.[4,11] However, in the present BCPs (with a molecular weight that is 20 times higher) the microdomain orientations change by about 90°.

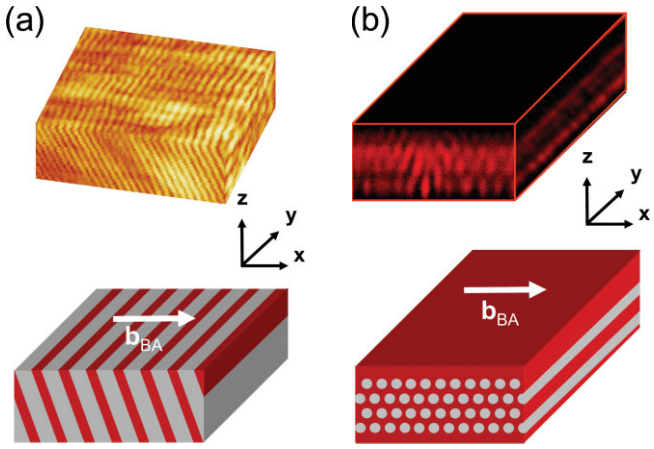

Figure 2. 3D reconstruction of reflection-mode LSCM images of highly ordered a) lamellar and b) cylindrical PS-*b*-PI BCPs in thin films obtained from the DS process. 3D imaging revealed that lamellae were tilted by about 60° to the fast-growth direction of BA and cylindrical microdomains were hexagonally packed in the *xz*-plane. Corresponding schematics with the direction of BA crystallization are also shown.

In the DS process, the symmetry-breaking external field inducing the microdomain orientation is a concentration gradient of the BCP molecules generated by the directional crystallization of the BA solvent. Figure 3 shows schematic diagrams of the BCP concentration profile during the DS process along the fast-growth direction ($\mathbf{b}_{BA}$) of BA for a) high and b) low molecular weight BCPs, in which the *y*-axis is the concentration (ϕ) of dissolved BCPs and the *x*-axis is the spatial coordinate along $\mathbf{b}_{BA}$. Above the melting temperature of BA ($T_{m,BA} \sim 123$ °C), the solution of BCPs in BA is a homoge-

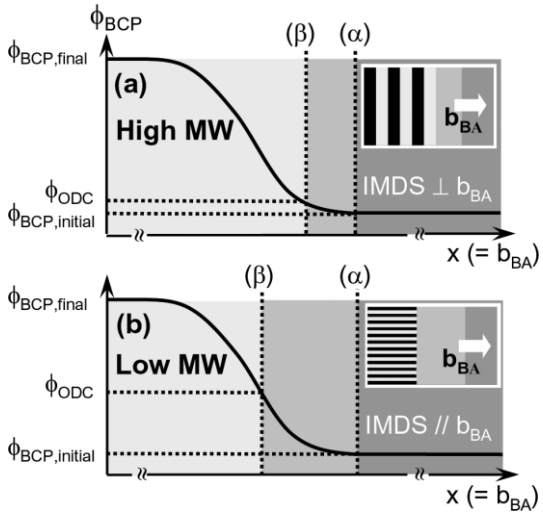

Figure 3. Schematic diagrams showing the concentration profile of BCP (ϕ_{BCP}) along $\mathbf{b}_{BA}$, the fast-growth direction of benzoic acid (BA) crystals during the DS process for a) high and b) low molecular weight (MW) BCP samples. The dotted lines represent the BA crystallization front (α) and BCP microphase separation front (β). The insets show schematics of corresponding microdomain orientations with respect to $\mathbf{b}_{BA}$ induced during the DS process.

neous liquid and the dissolved BCP chains are in a disordered state below the order–disorder transition concentration (ϕ_{ODC}). When the temperature is dropped below the $T_{m,BA}$, directional growth of BA crystals is initiated and simultaneously, the BCP concentration in the remaining liquid increases with directional extraction of solvent along the fast-growth direction of the solvent crystal. As the directional crystallization of BA proceeds further, the BCP concentration also increases and eventually reaches the ϕ_{ODC}, at which microphase separation of the BCP domains is initiated. After the onset of microphase separation at the phase separation boundary, the BCP concentration continues to increase and reaches the value of pure BCP ($\phi = 1.0$) as the remaining BA molecules diffuse out of the polymer and crystallize onto the essentially pure BA domains.

The molecular weight dependent microdomain orientation in the DS process can be understood in terms of a combination of the following three physical factors: i) order–disorder transition concentration (ϕ_{ODC}), ii) diffusivity of BCP molecules in solution, and iii) solubility of the PS and PI block unit with respect to BA. All of these factors have a strong molecular weight dependence and may play important roles during the course of microphase separation. Scaling laws for semidilute solutions suggest that the order–disorder transition of A–B diblock copolymer varies as: $\phi_{ODC} \sim (\chi N)^{-1/1.59}$, where χ is the Flory–Huggins interaction parameter, and N is the total degree of polymerization.[12,13] Thus, ϕ_{ODC} scales as $N^{-0.62}$ at a fixed temperature. Therefore, the order–disorder transitions for the present high molecular weight BCP systems occur at much lower concentrations than that for the low molecular weight BCPs because of the factor of 20 difference in the BCP molecular weight. As mentioned earlier, while a solvent (BA) crystallizes in the DS process, a directional extraction of the solvent generates a concentration gradient (i.e., $d\phi/dx$ in Fig. 3) along the solidification direction of the BA. Assuming that the growth velocity of the BA crystals and the resulting concentration profile are the same for high and low molecular weight BCPs, then the order–disorder concentration of high molecular weight BCP is reached much faster and the BCP microphase separation front (vertical line β in Fig. 3a) is much closer to the BA crystallization front (vertical line α in Fig. 3a) than for low molecular weight BCPs (Fig. 3b). The diffusion coefficient also strongly depends on molecular weight of BCPs. According to scaling laws for BCP solutions, the diffusion coefficient (D) of BCP in solution scales as $N^{-0.85}$ (in a semidilute regime with an athermal solvent),[14] and hence the high molecular weight BCPs in the present study should have a much lower diffusion coefficient than the previously studied low molecular weight BCPs. During microphase separation, the system will tend to minimize the interfacial free energy at the phase separation front. As the ordered BCP phase grows, the increment of interfacial free energy per unit growth is minimized if the interface between different phases grows perpendicular to the phase separation front. The previous results obtained from the relatively low molecular weight BCPs correspond to this case, in which the IMDSs are aligned perpendicular to the phase separation front (or parallel to $\mathbf{b}_{BA}$). On the other hand, if a BCP has sufficiently high molecular weight and thus has a rather low diffusion coefficient, the microphase separation is essentially a diffusion-controlled process and the BCP molecules cannot adopt the morphology of minimum interfacial energy because of kinetic limitations. The order–disorder transition, which occurs relatively earlier as a result of the relatively low value of the ϕ_{ODC} in the high molecular weight case, also contributes to this diffusion-controlled process for high molecular weight BCP samples.

Another physical factor which may influence the ordering behavior in the DS process is the solubility of PS-*b*-PI BCP in BA. The repeating PS monomeric unit should have a higher solubility in BA than the PI unit because of the similar chemical structure between styrene and benzoic acid. In BCP solution, the solubility of each block strongly depends on its molecular weight and its solubility parameter with respect to a solvent. As the concentration of high molecular weight block copolymer increases with the crystallization of BA, the PI block, which has a poorer solubility in BA, reaches the solubility limit in BA faster than the PS block. If this is the case, we can envision that under the diffusion-controlled process for high molecular weight BCPs, the PI block tends to phase separate first and the PS block follows, which produces the ordered structures where the IMDSs are aligned perpendicular to the fast-growth direction of BA crystal. Such perpendicularly ordered IMDSs with respect to the microphase growth direction were also previously observed in surface-induced microphase separation of a BCP melt in a temperature gradient,[15,16] and blends in a concentration gradient,[17] where the phase separation of one block is initiated because of the preferential wetting of the block to the substrate, and the microphase separation of the other block follows along the direction of the field gradient, resulting in the perpendicularly oriented domains.

In summary, highly oriented thin-film microdomain patterns of ultrahigh molecular weight BCPs having lamellar and cylindrical morphologies have been successfully created over a large area via directional solidification of a solvent. Interesting ordered textures of ultrahigh molecular weight BCPs were characterized by means of 3D optical LSCM imaging. The dramatic difference in the microdomain orientation obtained from ultrahigh molecular weight BCPs versus low molecular weight BCPs can be understood by diffusion- and solubility-controlled microphase separation of BCPs in solution during the directional extraction of the crystallizable solvent. These ultrahigh molecular weight BCP patterns have a domain size comparable to visible wavelengths and can be potentially used for fabricating useful thin-film photonic structures.[5,18]

Experimental

The ultrahigh molecular weight PS-*b*-PI diblock copolymers having lamellar and cylindrical morphologies were anionically synthesized by sequential addition of styrene and isoprene monomers to a mixed cy-

ADVANCED MATERIALS

clohexane/benzene solvent [18]. Molecular weights and compositions of the BCPs were 8.4×10^5 g mol^{-1} (polydispersity index (PDI): 1.08), 57:43 (PS/PI, w/w) for the lamellar-forming BCP (SI_{LAM}) and 1.15×10^6 g mol^{-1} (PDI: 1.05), 22:78 (PS/PI, w/w) for the cylinder-forming BCP (SI_{CYL}) as determined by gel permeation chromatography (GPC) and NMR analysis. In order to prepare highly oriented BCP samples in thin films, the directional solidification method with benzoic acid (BA) was applied as described in previous studies [11, 19]. Once the sample cooled down to room temperature, it was analyzed by reflection-mode LSCM (Leica TCS SPII) using a 488 nm probe laser beam without further treatment. Since the PS-*b*-PI BCP does not contain a fluorophore, reflection signals of the probe light were scanned for every LSCM image through an oil immersion objective lens (Leica, HCX PL APO 63 ×/1.40-0.60).

Received: April 6, 2006
Final version: August 9, 2006
Published online: September 21, 2006

[1] Y. Huang, C.-Y. Chiang, S. K. Lee, Y. Gao, E. L. Hu, J. De Yoreo, A. M. Belcher, *Nano Lett.* **2005**, *5*, 1429.
[2] P. Jiang, J. F. Bertone, V. L. Colvin, *Science* **2001**, *291*, 453.
[3] M. P. Stoykovich, M. Mueller, S. O. Kim, H. H. Solak, E. W. Edwards, J. J. de Pablo, P. F. Nealey, *Science* **2005**, *308*, 1442.
[4] C. Park, J. Yoon, E. L. Thomas, *Polymer* **2003**, *44*, 6725.
[5] J. Yoon, W. Lee, E. L. Thomas, *MRS Bull.* **2005**, *30*, 721.
[6] A. Urbas, Y. Fink, E. L. Thomas, *Macromolecules* **1999**, *32*, 4748.
[7] T. Deng, C. Chen, C. Honeker, E. L. Thomas, *Polymer* **2003**, *44*, 6549.
[8] A. M. Urbas, M. Maldovan, P. DeRege, E. L. Thomas, *Adv. Mater.* **2002**, *14*, 1850.
[9] K. J. Halbhuber, K. Konig, *Ann. Anat.* **2003**, *185*, 1.
[10] T. Wilson, C. J. R. Sheppard, *Theory and Practice of Scanning Optical Microscopy*, Academic, San Diego, CA **1984**.
[11] C. Park, C. De Rosa, E. L. Thomas, *Macromolecules* **2001**, *34*, 2602.
[12] J. F. Joanny, L. Leibler, R. Ball, *J. Chem. Phys.* **1984**, *81*, 4640.
[13] D. Broseta, L. Leibler, J. F. Joanny, *Macromolecules* **1987**, *20*, 1935.
[14] M. Rubinstein, R. H. Colby, *Polymer Physics*, Oxford University Press, New York **2003**.
[15] T. Hashimoto, J. Bodycomb, Y. Funaki, K. Kimishima, *Macromolecules* **1999**, *32*, 952.
[16] J. Bodycomb, Y. Funaki, K. Kimishima, T. Hashimoto, *Macromolecules* **1999**, *32*, 2075.
[17] S. Koizumi, H. Hasegawa, T. Hashimoto, *Macromolecules* **1994**, *27*, 6532.
[18] A. C. Edrington, A. M. Urbas, P. DeRege, C. X. Chen, T. M. Swager, N. Hadjichristidis, M. Xenidou, L. J. Fetters, J. D. Joannopoulos, Y. Fink, E. L. Thomas, *Adv. Mater.* **2001**, *13*, 421.
[19] C. De Rosa, C. Park, E. L. Thomas, B. Lotz, *Nature* **2000**, *405*, 433.

